ISSN 1063-7834, Physics of the Solid State, 2008, Vol. 50, No. 3, pp. 515–524. © Pleiades Publishing, Ltd., 2008.
Original Russian Text © I.N. Flerov, V.D. Fokina, A.F. Bovina, E.V. Bogdanov, M.S. Molokeev, A.G. Kocharova, E.I. Pogorel'tsev, N.M. Laptash, 2008, published in Fizika Tverdogo Tela, 2008, Vol. 50, No. 3, pp. 497–506.

LATTICE DYNAMICS AND PHASE TRANSITIONS

Mechanism and Nature of Phase Transitions in the $(NH_4)_3MoO_3F_3$ Oxyfluoride

I. N. Flerov[a], V. D. Fokina[a], A. F. Bovina[a], E. V. Bogdanov[a], M. S. Molokeev[a], A. G. Kocharova[a], E. I. Pogorel'tsev[b], and N. M. Laptash[c]

[a] *Kirensky Institute of Physics, Siberian Branch, Russian Academy of Sciences, Akademgorodok, Krasnoyarsk, 660036 Russia*
e-mail: flerov@iph.krasn.ru
[b] *Polytechnic Institute, Siberian Federal University, ul. Kirenskogo 26, Krasnoyarsk, 660074 Russia*
[c] *Institute of Chemistry, Far East Division, Russian Academy of Sciences, pr. Stoletiya Vladivostoka 159, Vladivostok, 690022 Russia*

Received July 18, 2007

Abstract—The temperature dependences of the heat capacity, the unit cell parameter, and the permittivity for the $(NH_4)_3MoO_3F_3$ cryolite (space group $Fm\bar{3}m$) are investigated. It is revealed that the compound undergoes ferroelectric and ferroelastic structural phase transitions at temperatures of 297 and 205 K, respectively. The mechanism of structural distortions is discussed in terms of the entropy parameters, pressure–temperature phase diagrams, and electron density maps for critical atoms. An analysis is made of the influence of the cation size and shape on the phase transitions in oxyfluorides of the general formula $A_2A'MO_3F_3$ (A, A' = NH_4, K; M = Mo, W).

PACS numbers: 61.50.Ks, 65.40.Ba, 65.40.Gr

DOI: 10.1134/S1063783408030219

1. INTRODUCTION

Calorimetric and structural investigations of fluorine–oxygen compounds of the general formula $A_2A'WO_3F_3$ (A, A' = K, NH_4) [1, 2] have revealed that crystals of these compounds in high-temperature phases have a cubic symmetry of cryolite (elpasolite) with space group $Fm\bar{3}m$ ($Z = 4$) and, under cooling, undergo a sequence of single phase transitions. The structure of the $K_3WO_3F_3$ cryolite at room temperature is distorted (space group Cm) [3], and, under heating, this compound undergoes two structural transformations of the ferroelectric and ferroelastic nature at temperatures $T_1 = 452$ K and $T_2 = 414$ K [4]. Each transition is accompanied by a relatively small change in the entropy ($\Delta S_1 = 0.52R$, $\Delta S_2 = 0.35R$). This circumstance indicates that the structural distortions are associated with the small atomic displacements.

The presence of tetrahedral ammonium ions at the nonequivalent crystallographic positions 8c and 4b leads to a considerable decrease in the temperature stability of cubic and intermediate phases with a drastic narrowing of the range of the intermediate phase in the $(NH_4)_3WO_3F_3$ compound: $T_1 = 200.1$ K and $T_2 = 198.2$ K [1]. Moreover, the substitution of ammonium for potassium results in a disordering of structural units in the initial phase, and distortions in the structure of the $(NH_4)_3WO_3F_3$ compound upon phase transitions are attended by a substantial change in the entropy (Rln7.6), which is characteristic of order–disorder transformations.

A combination of spherical and tetrahedral cations (NH_4 cations at the 8c positions and K cations at the 4b positions) in the $(NH_4)_2KWO_3F_3$ compound leads to a related elpasolite structure having the same space group $Fm\bar{3}m$ [2]. However, this substitution of univalent cations is accompanied by a significant change in the parameters of structural distortions: unlike cryolites, the $(NH_4)_2KWO_3F_3$ oxyfluoride undergoes one second-order phase transition with a small change in the entropy ($\Delta S_0 = 0.56R$). Furthermore, it turned out that the stability loss temperature of the initial phase ($T_0 = 234.5$ K) in the elpasolite is higher than the corresponding temperature in the $(NH_4)_3WO_3F_3$ cryolite. This did not correspond to the regularity which, up to now, was violated in no case in series of oxyfluorides $A_2A'MO_3F_3$ (A_2, A' = Cs, Rb, K; M = W, Mo) [4]. In order to elucidate the question as to whether the presence of the ammonium cation at the 8c position is responsible for the above circumstance, we investigated the $(NH_4)_2KMoO_3F_3$ elpasolite [5]. It was established that the substitution Mo $\longrightarrow$ W leads to a first-order transition in the $(NH_4)_2KMoO_3F_3$ elpasolite but only slightly affects the stability temperature of the cubic structure with space group $Fm\bar{3}m$: the molybdenum elpasolite undergoes the phase transition at 241.5 K. In this case,

the entropy of the transition in the $(NH_4)_2KMoO_3F_3$ elpasolite is $\Delta S_0 = R\ln 4.8$, which considerably exceeds the entropy of the transition in the tungsten analog ($\Delta S_0 = R\ln 1.8$) and suggests that ordering processes occur in the structure due to the phase transition. Moreover, unusual hysteresis and relaxation effects were revealed in the study of the heat capacity of the $(NH_4)_2KMoO_3F_3$ elpasolite: the temperature of the phase transition in this compound depended substantially on the prehistory of the sample. The compound could be transferred to a stable state by "annealing" at room temperature for 10–15 h. The regions of metastable states were found in the p–T phase diagram of the crystal over a wide range of temperatures and pressures.

Since similar effects were observed neither in the study of the heat capacity nor in phase diagrams of related tungsten oxyfluorides, we could assume that the aforementioned specific features are associated with the presence of the molybdenum atom instead of the tungsten atom in the structure. This can seem to be strange because the ionic radii of tungsten and molybdenum are very close to each other and equal to 0.59 and 0.60 Å, respectively. However, even Peraudeau et al. [6] noted that the replacement of the tungsten atom by the molybdenum atom results in an increase in the degree of covalency of the M–O bond and this substantially affects, in particular, the temperature of the transition from the cubic phase in $A_3MO_3F_3$ (A = K, Rb, Cs; M = W, Mo) cryolites. In order to confirm or refute this assumption, in the present work, we investigated the temperature dependences of the heat capacity, the unit cell parameter, and the permittivity and analyzed the p–T phase diagram for the ammonium oxyfluoride $(NH_4)_3MoO_3F_3$.

2. SYNTHESIS, IDENTIFICATION OF THE SAMPLES, AND PRELIMINARY RESEARCHES

Ammonium molybdate, which was the initial compound for the synthesis of the $(NH_4)_3MoO_3F_3$ ammonium oxyfluoride, was prepared according to the reaction

$$MoO_3 + 2NH_4OH_{exc} \longrightarrow (NH_4)_2MoO_4 + H_2O.$$

After filtration and drying in air, the $(NH_4)_2MoO_4$ ammonium molybdate was mixed with NH_4OH. Then, HF was added in excess to the prepared mixture with vigorous stirring. The violent reaction

$$(NH_4)_2MoO_4 + 3HF_{exc} + NH_4OH \longrightarrow (NH_4)_3MoO_3F_3 + 2H_2O$$

resulted in the formation of a finely dispersed powder of the compound under investigation.

Single crystals were synthesized using another procedure. The $(NH_4)_2MoO_4$ ammonium molybdate also served as the initial compound. The addition of a concentrated NH_4F solution (40%) to an aqueous solution of the ammonium molybdate led to the formation of a heavy white precipitate, which was a mixture of ammonium oxofluoromolybdates $(NH_4)_3MoO_3F_3$ and $(NH_4)_2MoO_3F_2$. The prepared precipitate was dissolved in water with addition of a small amount of HF and an excess amount of NH_4F. The solution was heated and hydrolyzed by an ammonia solution to the appearance of a white precipitate (pH 7–8), which was a finely crystalline $(NH_4)_3MoO_3F_3$. The precipitate was filtered off, and larger crystals of the complex, predominantly in the form of hexagonal plates, were grown from the mother solution upon slow evaporation in air. Further crystallizations resulted in the formation of small single crystals in the form of regular octahedra.

The $(NH_4)_3MoO_3F_3$ crystals were analyzed for the ammonium, molybdenum, and fluorine contents. The ammonium content was determined by the Kjeldahl method, and the molybdenum and fluorine contents were determined by pyrohydrolysis (with the use of one sample). The calculated and experimental (in parentheses) contents are as follows: NH_4, 21.2 (21.2 ± 0.3) wt %; Mo, 37.6 (37.8 ± 0.5) wt %; and F, 22.4 (22.0 ± 0.5) wt %.

The samples were characterized on a DRON-2 x-ray diffractometer. It was established that, at 291 K (the temperature of the environment in the course of investigations), the compound has a cubic symmetry with the unit cell parameter $a_0 = 9.131$ Å and belongs to the cryolite–elpasolite family. However, the polarization-optical investigations revealed that the crystals at this temperature are not optically isotropic and undergo a phase transition to a cubic phase upon heating to temperatures above ~291–295 K.

The disagreement between the results of the structural and optical experiments was explained in the study of the heat capacity of the $(NH_4)_3MoO_3F_3$ compound on a DSM-2M differential scanning microcalorimeter (DSM). The measurements were performed upon heating and cooling (the scanning rate was equal to 8 K/min) in the temperature range 110–350 K. We investigated several samples obtained in each crystallization series prepared by different methods described above. The sample weight amounted to 0.10–0.12 g. It was found that, upon heating, the heat capacity of all samples is characterized by an anomaly in the form of a sharp peak. The temperature of the maximum, which was interpreted as the phase transition temperature, varied from sample to sample in the range T_1 = 291–295 K.

Figure 1 depicts the experimental temperature dependence of the excess heat capacity ΔC_p for one of the samples. The excess heat capacity was determined as the difference between the total molar heat capacity of the compound and its lattice component. A significant hysteresis in the temperature of the heat capacity maximum ($\delta T_1 \approx 13$ K) found in the thermal cycling experiments suggests that the transition is a first-order transformation. The enthalpy associated with the phase

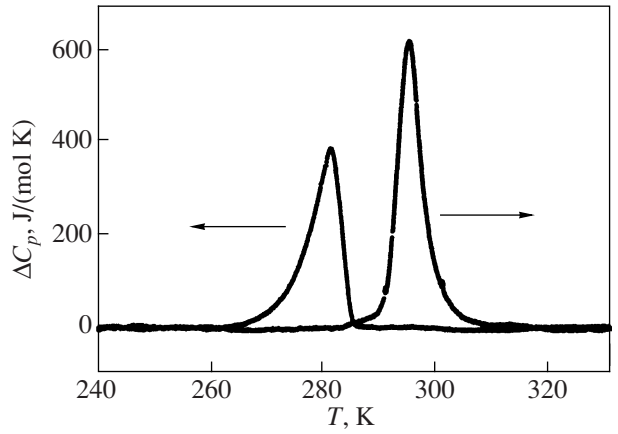

Fig. 1. Temperature dependence of the excess heat capacity measured with a differential scanning microcalorimeter for the $(NH_4)_3MoO_3F_3$ compound during heating and cooling.

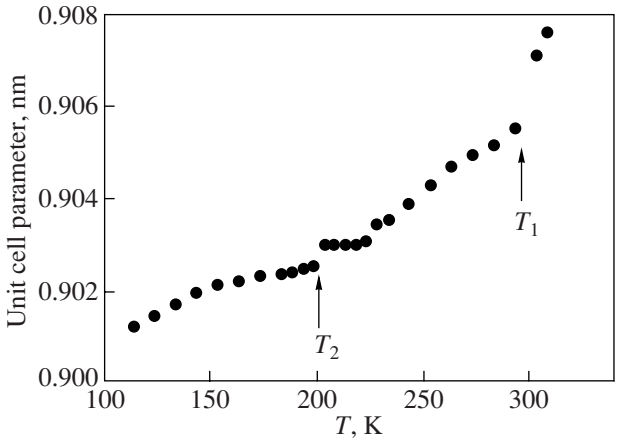

Fig. 2. Temperature dependence of the unit cell parameter of the $(NH_4)_3MoO_3F_3$ compound.

transition $\Delta H_1 = 3200 \pm 300$ J/mol was determined by integrating the function $\Delta C_p(T)$.

No noticeable differences between the x-ray diffraction patterns of the initial and low-temperature phases were revealed in temperature x-ray investigations of the $(NH_4)_3MoO_3F_3$ compound. This circumstance is the main factor that allows us to assign cubic symmetry to the $(NH_4)_3MoO_3F_3$ sample at room temperature. The presence of the phase transition was identified from an anomalous behavior of the unit cell parameter at a temperature of 297 K (Fig. 2). Furthermore, these results indicate that an anomalous behavior of the unit cell parameter is also observed in the range of 205 K. However, no anomalies in this temperature range were reliably revealed in the temperature dependence of the heat capacity measured by the DSM method.

3. HEAT CAPACITY AND THE *p–T* PHASE DIAGRAM

At the second stage, the heat capacity of the $(NH_4)_3MoO_3F_3$ compound was studied by adiabatic calorimetry. The sample (weight, 0.90 g) under investigation was placed in a copper container. Then, the container in an inert helium atmosphere was hermetically sealed in an indium cell, which, in turn, was placed in accessories with a heater. The heat capacity of the system was measured under conditions of continuous (dT/dt = 0.15 K/min) and discrete (ΔT = 2.5–3.0 K) heatings. The immediate vicinities of the phase transition were investigated using quasi-static thermograms at mean heating and cooling rates $|dT/dt| \approx 0.02$ K/min. The heat capacity of the accessories (heater, copper and indium cells) was measured in a separate experiment.

The temperature dependence of the molar heat capacity at constant pressure for the $(NH_4)_3MoO_3F_3$ compound according to the calorimetric measurements is shown in Fig. 3a. It can be seen from this figure that, apart from the pronounced heat capacity anomaly (corresponding to the phase transition) revealed with the DSM method, the temperature dependence $C_p(T)$ exhibits one more anomaly in the low-temperature range. The temperature of this anomaly is in good agreement with the temperature of the anomalous behavior of the unit cell parameter (Fig. 2). This suggests that, at the given temperature, there is a phase transition that could not be reliably revealed by the DSM method due to its lower sensitivity. The phase transition temperatures refined in measurements with the adiabatic calorimeter are $T_1 = 297.14 \pm 0.05$ K and $T_2 = 205.4 \pm 0.2$ K.

The dashed line in Fig. 3a indicates the temperature dependence of the lattice heat capacity, which was determined by a polynomial approximation of the experimental data outside the range of the anomalies. It can be seen from Fig. 3a that the anomalous contribution to the heat capacity is observed over a wide range

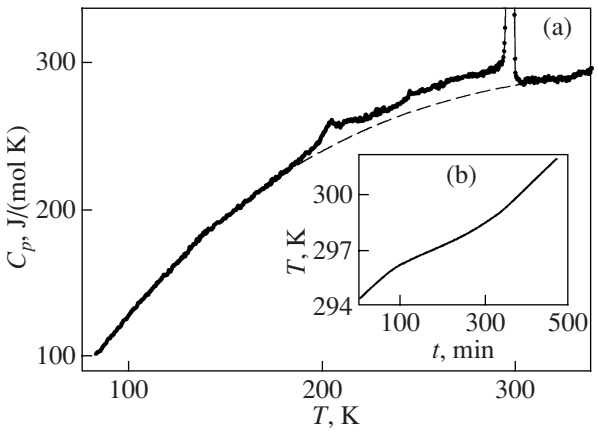

Fig. 3. (a) Temperature dependence of the heat capacity for the $(NH_4)_3MoO_3F_3$ oxyfluoride (the dashed line indicates the lattice heat capacity) and (b) thermogram measured under heating.

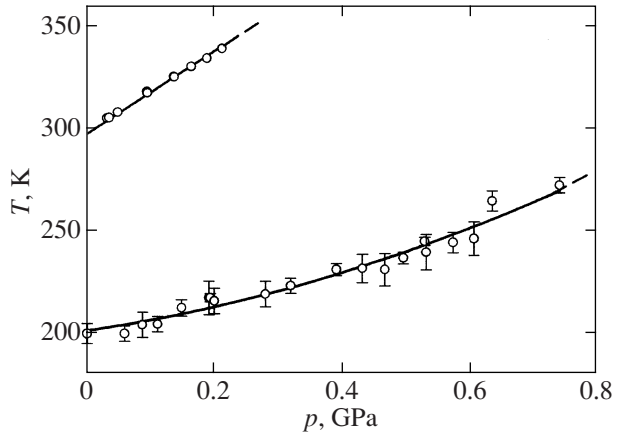

Fig. 4. The p–T phase diagram of the $(NH_4)_3MoO_3F_3$ oxyfluoride.

of temperatures below T_1. A weak temperature dependence is a characteristic feature of the anomalous heat capacity in the intermediate phase. Moreover, it is clearly seen from Fig. 3a that the dependence $\Delta C_p(T)$ exhibits a "hump-shaped" anomaly over a wide range of temperatures. However, no noticeable features in the behavior of the unit cell parameter at the corresponding temperatures were found in the x-ray experiments.

The above circumstance complicates the unique determination of the enthalpies of the phase transitions. However, the ratio between these enthalpies for the transitions at the temperatures T_1 and T_2 is such that the quantities ΔH_i can be calculated by integrating the function $\Delta C_p(T)$ in the temperature ranges 220–305 and 180–220 K. In this case, the changes in the enthalpy are as follows: $\Delta H_1 = 3800 \pm 240$ J/mol and $\Delta H_2 = 300 \pm 30$ J/mol. The corresponding entropies were determined by integrating the function $(\Delta C_p/T)(T)$: $\Delta S_1 = 13.3 \pm 0.8$ J/(mol K) and $\Delta S_2 = 1.5 \pm 0.15$ J/(mol K). The phase transition from the cubic phase in the cryolite is a first-order transformation in agreement with the data on the heat capacity obtained by the DSM method and the unit cell parameters. The results of investigations in the vicinity of this transition at low rates of change in the temperature in the quasi-static thermography regime (Fig. 3b) permitted us to refine the value of the temperature hysteresis $\delta T_1 = 6$ K. Although this value is less than that determined from the DSM measurements, it appears to be comparable to the corresponding hysteresis for the $(NH_4)_2KMoO_3F_3$ elpasolite [5],

The specific feature of the behavior of the heat capacity in the vicinity of the phase transition at T_1 is that the heat capacity does not depend on the heating rate of the sample. When measuring the heat capacity with the use of the quasi-static thermograms at a heating rate of 0.02 K/min, neither the shape nor the magnitude of the anomaly at T_1 differ from those obtained in measurements performed at a rate of 0.15 K/min. Most likely, this is a consequence of a rather poor quality of the crystal. The above explanation is confirmed by the smearing of the latent heat over a very wide range of temperatures (~3 K, Fig. 3b). As a result, the latent heat of the transition can be determined only approximately: $\delta H_1 \approx 2700$ J/mol.

The influence of the hydrostatic pressure on the temperatures and the sequence of the phase transitions in the $(NH_4)_3MoO_3F_3$ compound was studied by differential thermal analysis (DTA) under pressure. A sensitive element of a thermocouple consisted of copper–germanium–copper electrodes connected in series. A pressure as high as 0.75 GPa was produced in a cylinder–piston camber connected to a multiplier. A transformer oil was used as the pressure-transferring medium. The pressure in the chamber was measured on a manganin resistance pressure gauge, and the temperature of the sample under investigation was measured using a copper–constantan thermocouple. The errors of measurements were equal to $\pm 10^{-3}$ GPa and ± 0.3 K, respectively. The positions of the phase boundaries in the p–T phase diagram were determined upon increase and decrease in the pressure with a reasonable reproducibility.

The experimental p–T phase diagram of the compound under investigation is depicted in Fig. 4. The DTA method used enabled us to reveal reliably the anomalies associated with the phase transitions at the temperatures T_1 and T_2. However, no features associated with the hump-shaped anomaly observed in the temperature dependence of the heat capacity at constant pressure were found in the DTA curve.

An increase in the pressure leads to an increase in the temperatures of both transitions, and the dependences $T(p)$ are described by the relationships $T_1 = 297.1 + 202p$ and $T_2 = 204.3 + 46p + 63p^2$. It can be seen that the slopes of the phase boundaries dT_1/dp and dT_2/dp differ substantially. Therefore, under pressure, the temperature range of stability of the initial cubic range decreases, whereas the temperature ranges of the distorted phases increase. No triple points were revealed in the phase diagram.

4. CRYSTAL STRUCTURE

The analysis of the crystallographic parameters for the $(NH_4)_3MoO_3F_3$ cryolite was carried according to the procedure described in our earlier work [5] for the $(NH_4)_2KMoO_3F_3$ elpasolite. The data on the isostructural compound $(NH_4)_3WO_3F_3$ [2] were used as the initial parameters of the structure model. The Mo atom replaces the W atom at the (0; 0; 0) position. The O (F) atoms are statistically disordered over the crystal volume and occupy the (x; 0; 0) positions with an occupancy of 0.5. The x coordinate was refined to be –0.1852(8). The thermal parameters of the Mo and N atoms were refined in the isotropic approximation. The

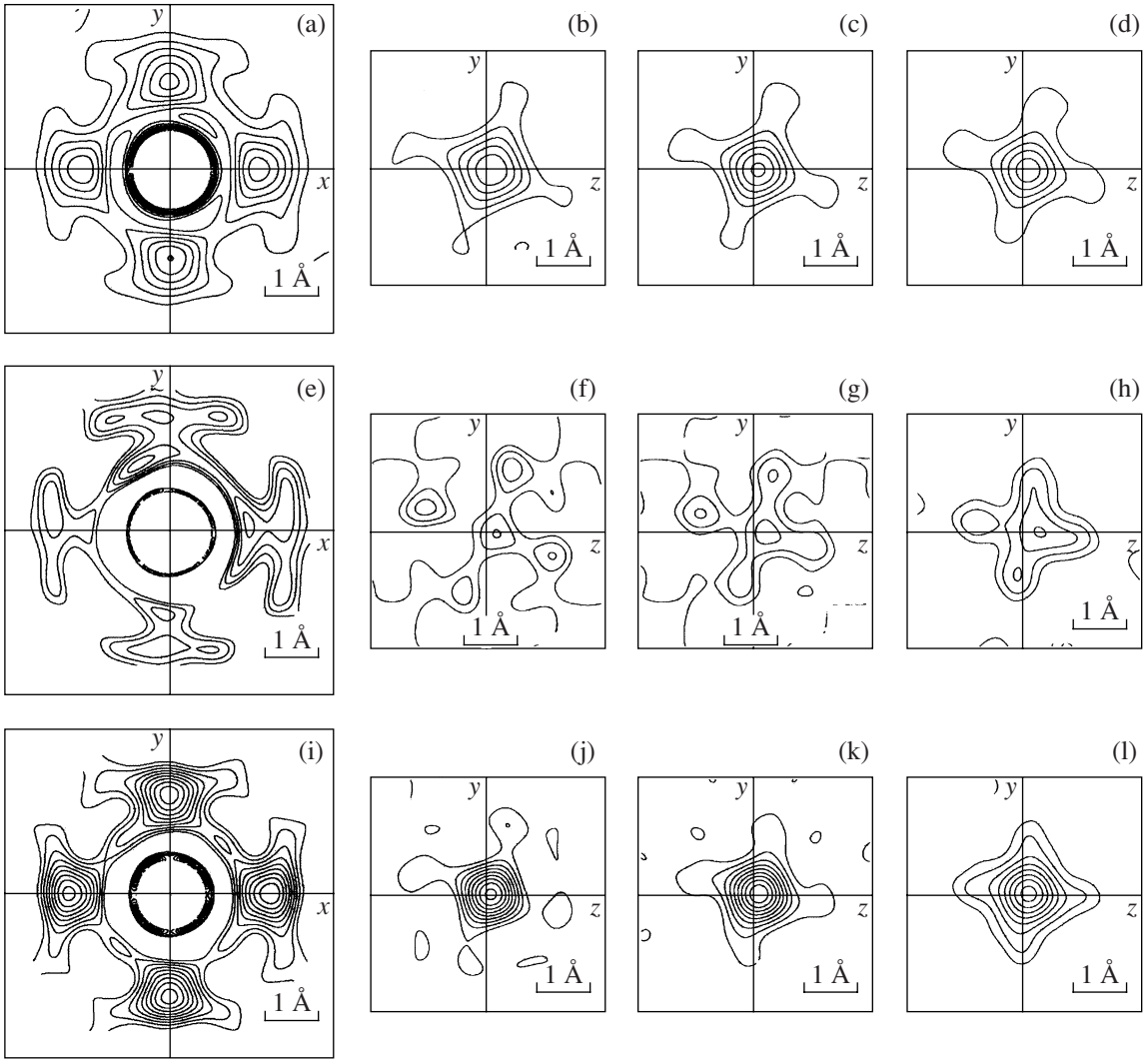

Fig. 5. Electron density maps (step, 0.4 e/Å^3) for the (a–d) $(NH_4)_3MoO_3F_3$, (e–h) $(NH_4)_3WO_3F_3$ [2], and (i–l) $(NH_4)_2KMoO_3F_3$ [5] compounds through the center of the (a, i) MoO_3F_3 and (e) WO_3F_3 octahedra ($z = 0$) and the corresponding coordinates (c, g, k) x, (b, f, j) $x - 0.02$, and (d, h, l) $x + 0.02$ for the O (F) atoms.

coordinates of the H atom were fixed at a distance of 0.8 Å from the N atom and, as in the case of the thermal parameter, were not refined. The results of the structure refinement are presented in Table 1.

The electron density maps for the central atom and the ligands forming the MoO_3F_3 octahedron in the structure of the $(NH_4)_3MoO_3F_3$ compound are shown in Fig. 5. A set of cross sections passing through the center of the octahedron and only through its vertices clearly demonstrates a pronounced anisotropy of vibrations of the F (O) atoms. In this respect, their thermal parameters were subsequently refined in the anisotropic

Table 1. Parameters of the data collection and structure refinement for the $(NH_4)_3MoO_3F_3$ compound

Space group	a, Å	V, Å^3	2θ angle range, deg	Number of Bragg reflections	Number of parameters refined	R_p, %	R_{wp}, %	R_B, %
$Fm\bar{3}m$	9.1315(1)	761.42(1)	15–110	41	7	22.4	25.3	6.99

Note: a is the unit cell parameter; V is the unit cell volume; and R_p, R_{wp}, and R_B are the profile reliability factor, the weighted profile reliability factor, and the Bragg reliability factor, respectively.

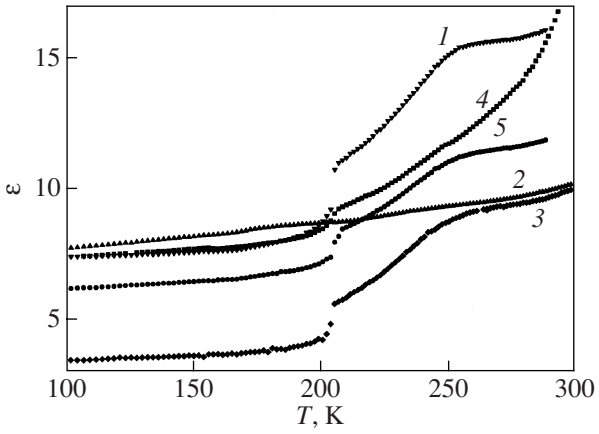

Fig. 6. Temperature dependences of the permittivity ε for (*1–3*) the $(NH_4)_2WO_2F_4$ single crystal along the directions perpendicular to the (*1*) (100), (*2*) (010), and (*3*) (001) planes and (*4*) the "quasi-ceramic" sample. (*5*) Temperature dependence of the averaged permittivity ε for the single crystal.

approximation. The anisotropic thermal parameters for the ligands are U_{11} = 0.026(1) Å^2 and $U_{22} = U_{33}$ = 0.045(1) Å^2. The atomic coordinates, isotropic thermal parameters, and site occupancies are listed in Table 2.

Undeniably, it is interesting to compare the electron density distributions in the structures of the $(NH_4)_3MoO_3F_3$ cryolite and the related compounds $(NH_4)_3WO_3F_3$ [2] and $(NH_4)_2KMoO_3F_3$ [5] (Fig. 5). On the one hand, the substantial difference between the anisotropies of ligand vibrations in the molybdenum and tungsten elpasolites (revealed in our previous work [5]) is also characteristic of the cryolite structures. On the other hand, it is evident that these differences in the molybdenum elpasolite and the molybdenum cryolite are minimum. A comparison of a number of cross sections of the molybdenum and tungsten octahedra (Fig. 5) shows a different degree of anharmonicity of the F (O) atoms in the cryolites. A similar situation was observed when comparing the electron density distributions in the elpasolite structures [5].

Table 2. Atomic coordinates, isotropic thermal parameters (B_{iso}), and site occupancies (p) in the structure of the $(NH_4)_3MoO_3F_3$ compound

Atom	p	X	Y	Z	B_{iso}, Å^2
Mo	1.0	0	0	0	5.6(1)
N	1.0	0.5	0.5	0.5	4.7(3)
N	1.0	0.25	0.25	0.25	6.7(3)
H	1.0	0.198	0.198	0.198	1.0
F	0.5	0.1852(8)	0	0	12.9*
O	0.5	0.1852(8)	0	0	12.9*

* The thermal parameter was refined in the anisotropic approximation.

5. DIELECTRIC MEASUREMENTS

As was noted above, the $(NH_4)_3MoO_3F_3$ compound undergoes the first-order phase transition, which is not accompanied by substantial changes in the x-ray powder diffraction patterns. A similar situation was observed in preliminary investigations of phase transitions in the $K_3WO_3F_3$ compound: the transition from the cubic phase to the distorted ferroelectric phase did not reflect in the x-ray diffraction pattern [3]. This fact indicated that the appearance of the polarization is not associated with the significant transformation of the $K_3WO_3F_3$ structure. The above circumstances suggested that the polarization can appear in the $(NH_4)_3MoO_3F_3$ compound due to the phase transition. In this respect, we measured the temperature dependences of the permittivity of the cryolite under investigation. It should be noted that the corresponding investigations for ammonium-containing oxyfluorides have never been performed.

As was noted above, we did not succeeded in preparing the $(NH_4)_3MoO_3F_3$ cryolite in the form of bulk single crystals. Moreover, ceramic samples cannot be prepared using the traditional technique involving sintering at high temperatures due to the low decomposition temperature of the given compound (~400 K). The sole possibility was to attempt to study "quasi-ceramic" samples in the form of pressed pellets prepared without heat treatment. In order to verify the applicability of this approach to the determination of the permittivity, we carried out test studies with the use of the $(NH_4)_2WO_2F_4$ oxyfluoride grown in the form of sufficiently large single crystals and characterized by the ferroelastic transition from the orthorhombic phase (with space group *Cmcm*) to the triclinic phase (with space group $P\bar{1}$) in the range of 200 K [7, 8].

Plates ~1 mm thick were cut parallel to the (100), (010), and (001) planes of the $(NH_4)_2WO_2F_4$ crystal. Copper electrodes were applied through vacuum evaporation. The dependences ε(T) were measured on an E7-20 immittance meter at a frequency of 1 kHz in the temperature range 100–300 K upon heating at a rate of ~1 K/min. The temperature dependences of the permittivity measured along three principal directions of the crystal lattice are plotted in Fig. 6.

It was revealed that the quantities ε_a and ε_c at a temperature of 200 K (the temperature of the ferroelastic phase transition) are characterized by a stepwise increase, which is typical of first-order nonferroelectric phase transitions [9]. Furthermore, it is clearly seen from Fig. 6 that, in the temperature range 250–270 K, the dependences ε(T) (for two cuts) exhibit a pronounced kink. This specific feature correlates with the behavior of the heat capacity [7] and the birefringence [8] and can be associated with the pretransitional phenomena.

At the second stage, a finely dispersed powder was prepared from the single crystals. This powder was

pressed in the form of a cylindrical pellet 8 mm in diameter and 2.5 mm in height. The pellet was pressed without binding agent at a pressure of ~0.1 GPa. As for the single-crystal plates, we also used copper electrodes.

The temperature dependence of the permittivity ε for the quasi-ceramic sample (Fig. 6, curve *4*) exhibits specific features identical to those observed in the dependence ε(*T*) for the single-crystal samples: a jump at 200 K and a kink in the temperature range 250–270 K. The temperature dependence of the averaged permittivity for the $(NH_4)_2WO_2F_4$ single crystal is also depicted in Fig. 6 (curve *5*). The averaged permittivity was determined as the mean arithmetic $\Sigma\varepsilon_i/3$. It is clear that the dependence of the permittivity measured for the quasi-ceramic sample agrees reasonably with the dependence $(\Sigma\varepsilon_i/3)(T)$. This confirms the possibility of performing dielectric investigations of pressed powders prepared without heat treatment.

Quasi-ceramic samples of the $(NH_4)_3MoO_3F_3$ compound were prepared using the above technique. The dependences ε(*T*) were measured in the temperature range 100–315 K upon heating and cooling at rates of 1–2 K/min. It can be seen from Fig. 7a that, in the course of heating, the permittivity (ε = 8 at 100 K) increases over the entire temperature range under investigation and reaches a maximum $\varepsilon^{+}_{max} = 120$ at a temperature of 297 ± 0.2 K, which is in reasonable agreement with the temperature of the phase transition to the cubic phase according to the calorimetric measurements. In the cubic phase, the permittivity ε decreases and is equal to 100 at a temperature of 310 K.

Upon cooling, the maximum permittivity is considerably larger: $\varepsilon^{-}_{max} = 190$. This specific feature is characteristic of first-order phase transitions [9]. In the low-temperature phase, the cooling curve coincides with the heating curve at temperatures below 240 K. The revealed hysteresis of the transition temperature ΔT_1 = 11 K is in satisfactory agreement with that determined in the DSM measurements and turns out to be considerably larger than the hysteresis observed in the thermograms obtained at low rates of change in the temperature.

It should be noted that the dielectric losses increase in the range of the phase transition at the temperature T_1 (Fig. 7c). That is why the dielectric measurements were performed only to a temperature of 315 K.

The temperature dependence of the permittivity ε exhibits an anomalous behavior in the temperature range 200–210 K (Fig. 7b). This agrees satisfactorily with the temperature T_2 of the low-temperature phase transition revealed in the measurements of the heat capacity and the unit cell parameter. However, no noticeable changes in the behavior of the dependence ε(*T*) are observed in the temperature range corresponding to the hump-shaped anomaly of the heat capacity.

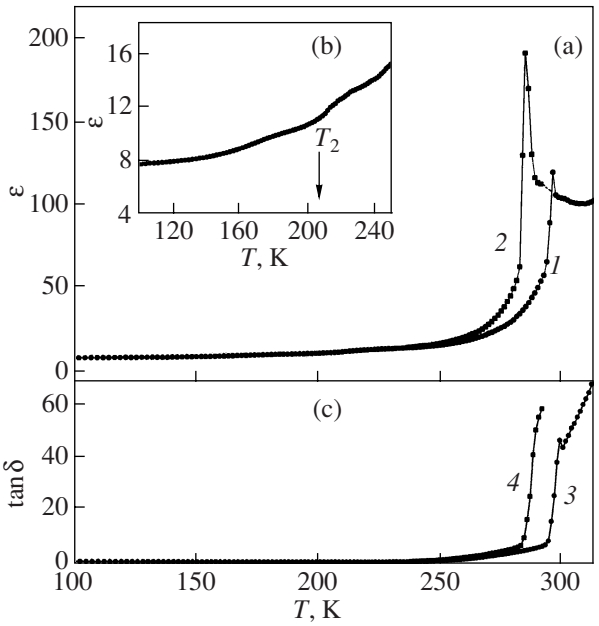

Fig. 7. Temperature dependences of (a, b) the permittivity ε (a) over a wide range of temperatures and (b) in the range 100–250 K and (c) the dielectric loss tangent tanδ for the $(NH_4)_3MoO_3F_3$ compound measured during (*1*, *3*) heating and (*2*, *4*) cooling.

6. DISCUSSION OF THE RESULTS

The performed investigations revealed that, as should be expected, the cation substitution $NH_4 \longrightarrow K$ in the molybdenum elpasolite does not lead to a change in the structure of the initial phase with space group $Fm\bar{3}m$ It should be noted that, in both molybdenum compounds $(NH_4)_3MoO_3F_3$ and $(NH_4)_2KMoO_3F_3$, the transition from the cubic phase is characterized by the latent heat. Moreover, the ratios between the latent heat and the total change in the enthalpy for these compounds are virtually identical: $\delta H_1/\Delta H_1 \approx 0.7$. This clearly indicates that the transitions under consideration are far from the tricritical point.

However, no hysteresis phenomena characteristic of the elpasolite in temperature and/or pressure cycling experiments [5] are observed for the physical properties of the cryolite. Furthermore, the structural distortion in the molybdenum cryolite occurs through the sequence of two phase transitions with a hypothetical triple point in the range of negative pressures. The initial slopes of the boundaries between the cubic and first distorted phase differ significantly not only in magnitude but also in the sign. This clearly indicates that the mechanisms of the corresponding phase transitions should differ from each other.

Let us consider the problems associated with the nature of the phase transitions revealed in the $(NH_4)_3MoO_3F_3$ compound. In the framework of the concepts following from the thermodynamic theory of

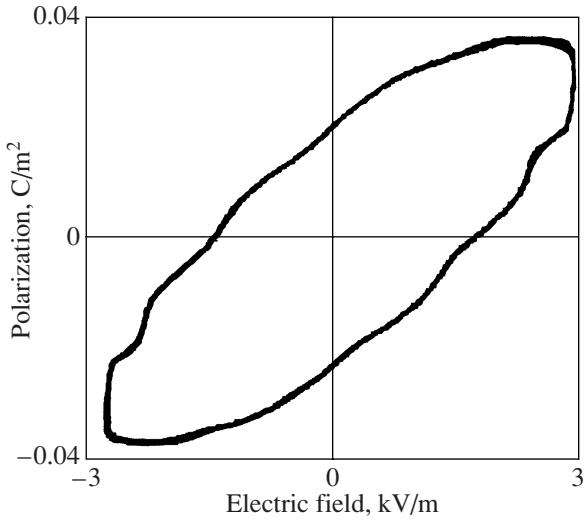

Fig. 8. Dielectric hysteresis loop for the $(NH_4)_3MoO_3F_3$ cryolite.

ferroelectricity [9], the behaviors of the permittivity in the vicinity of phase transitions in nonferroelectric crystals (for example, ferroelastics) and ferroelectrics differ substantially. For first-order ferroelastic transitions, the dependence $\varepsilon(T)$ is similar to those revealed for the crystals of the compounds $(NH_4)_2WO_2F_4$ (the transition at the temperature T_1) and $(NH_4)_3MoO_3F_3$ (the transition at the temperature T_2) (Figs. 6, 7). Since it is known from polarization-optical investigations that the transition in the $(NH_4)_2WO_2F_4$ compound is a ferroelastic transformation [8], we can make the same inference regarding the nature of the low-temperature transition in the $(NH_4)_3MoO_3F_3$ compound.

According to the theoretical concepts [9], the experimentally revealed behavior of the permittivity of the $(NH_4)_3MoO_3F_3$ cryolite over a wide range of temperatures and in the immediate vicinity of the temperature T_1 permits us to attribute the high-temperature transition to ferroelectric transformations. Actually, for the $(NH_4)_3MoO_3F_3$ compound (Fig. 7), as for ferroelectrics, the permittivity ε in the ferroelectric phase increases considerably below the transition temperature, sharply changes at T_1, and decreases at $T > T_1$. A similar behavior of the dependence $\varepsilon(T)$ was observed for the classical perovskite-like ferroelectric $BaTiO_3$ [10].

Most likely, we could expect a larger value of the permittivity ε at the point of the high-temperature phase transition in the $(NH_4)_3MoO_3F_3$ compound; however, the following circumstances should be taken into account. First, the measurements were carried out using the quasi-ceramic sample, i.e., along some averaged direction. Second, the pronounced first-order transition occurs at the temperature T_1. Therefore, the permittivity reaches only values of $\sim 10^2$, because the crystal transforms into a low-symmetry phase. Third, the density of the quasi-ceramic sample (1.87 g/mm^3) is significantly lower than the theoretical density calculated from the x-ray diffraction data (2.2 g/mm^3), and air filling holes between grains undeniably decreases the permittivity.

For the sample used for investigating the temperature dependence of the permittivity $\varepsilon(T)$, the polarization was measured at a frequency of 50 Hz and room temperature, i.e., in the immediate vicinity of the phase transition (T_1 – 4K). The dielectric hysteresis loop is shown in Fig. 8. A somewhat distortion (rounding) of the corners and a large area of the hysteresis loop can be associated with the following factors: first, the low frequency of the measurements [11], second, the low density of the sample, and, third, the high dielectric losses [12]. All factors can contribute for the quasi-ceramic sample under investigation; however, the main role is most likely played by the last factor. This inference is confirmed by the dependence $\tan\delta(T)$ (Fig. 7c): the dielectric losses are small in magnitude over a wide range of temperatures and increase drastically in the immediate vicinity of the temperature T_1.

The coercive field amounts to 1.75 kV/m, and the remanent and maximum polarizations are equal to 0.02 and 0.04 C/m^2, respectively.

A further analysis of the experimental data obtained for the $(NH_4)_3MoO_3F_3$ cryolite will be performed from the standpoint of the influence of substitutions of tetrahedral cations for spherical cations at the 4*a* position and the central atom at the position 4*b* in the MoO_3F_3 octahedron (Mo ⟶ W) on the properties and phase transitions of elpasolites (cryolites).

The temperature of the transition from the cubic phase in the $(NH_4)_3MoO_3F_3$ compound appears to be considerably higher than that in the $(NH_4)_2KMoO_3F_3$ elpasolite studied earlier in [5]. This experimental fact is in reasonable agreement with the specific feature of the ratio between these temperatures for oxyfluorides with univalent atomic cations in both crystallographic positions (4*a,* 8*c*) [4]: compared elpasolites, cryolites undergo phase transitions at higher temperatures. Therefore, the hypothesis regarding a significant influence of the covalency of *M*–O bonds on the temperature T_1 in oxyfluorides of the general formula $A_2A'MO_3F_3$ (M = Mo, W) [6] is most likely valid for structures containing tetrahedral cations and the effect observed for the $(NH_4)_2KWO_3F_3$ elpasolite [2] can be treated as an exception.

Moreover, the effect of the replacement of the central atom manifests itself in the thermodynamic properties and the difference between the specific features of the mechanisms of structural distortions. It can be seen from Fig. 9 that, unlike the tungsten compounds, the entropies of the transition from the cubic phase in both molybdenum oxyfluorides are close to each other and characteristic of order–disorder processes ($\Delta S_1 = R\ln 5$ for the $(NH_4)_3MoO_3F_3$ compound and $\Delta S_0 = R\ln 4.8$ for the $(NH_4)_2KMoO_3F_3$ compound [5]). Furthermore, the

entropy of the transition for the molybdates is considerably lower than that for the $(NH_4)_3WO_3F_3$ cryolite ($\Delta S = R\ln 7.6$ [1]).

According to the model concepts regarding the disorder in the cubic phase of elpasolites (cryolites) [12], the entropy of the transition can be governed by the ordering of MO_3F_3 octahedra, NH_4 tetrahedra, and spherical cations at the 8*c* positions. It should be kept in mind that, since the ferroelectric transitions from the cubic phase are necessarily associated with the displacements of the central atoms, these processes also contribute to the entropy.

The analysis of the electron density maps (Fig. 5) shows that, although the F (O) atoms in the structures of the $(NH_4)_2KMoO_3F_3$ and $(NH_4)_3MoO_3F_3$ compounds execute anisotropic vibrations, they, on average, occupy the position at the unit cell edge with a high probability as compared to the related compounds $(NH_4)_2KWO_3F_3$ and $(NH_4)_3WO_3F_3$ [2] and, as a result, seemingly cannot make a considerable contribution to the entropy of the transition. However, it is known that the symmetry of distorted phases of oxyfluorides with atomic cations, as a rule, is very low and associated with the superposition of ($\varphi\varphi\varphi$) rotations of the MoO_3F_3 octahedra around three axes of the initial cubic cell, as is the case, for example, in the structure of the $Na_3MoO_3F_3$ compound [13]. In this case, according to [12], the change in the entropy due to the structural distortion can be rather large: $3\Delta S_i \approx 0.6R$. There are no grounds to believe that the symmetry of distorted phases in ammonium-containing crystals is higher than monoclinic. At least, this was demonstrated in our previous work [3], in which we established that the $(NH_4)_2KWO_3F_3$ and $(NH_4)_2WO_3F_3$ compounds undergo transitions to the $P2_1/n$ phase, the model representation of which is associated with the ($\varphi\varphi\psi$) distortion [12]. Therefore, with allowance made for the above reasoning, we can argue that the contribution to the quantity ΔS_1 for molybdates can also be of the order of $0.6R$.

Since at least the $(NH_4)_3MoO_3F_3$ crystal according to our analysis undergoes the ferroelectric phase transition at the temperature T_1, there necessarily exists a contribution from the displacement of central atoms to the entropy. However, the corresponding entropy, as a rule, is low and amounts to no more than ~$0.1R$, as is the case, for example, in the classical ferroelectric $BaTiO_3$ [10].

Therefore, the contribution to the entropy of the transition minus the entropies associated with the octahedra rotations ($0.6R$) and the displacement of central atoms ($0.1R$) for both molybdates remains to be $\geq R\ln 2$. Since the tetrahedral cations at the 4*b* positions in the cryolite structure should be disordered, the above change in the entropy can be due to the ordering of these structural units. However, this explanation is inapplicable to the $(NH_4)_2KMoO_3F_3$ compound.

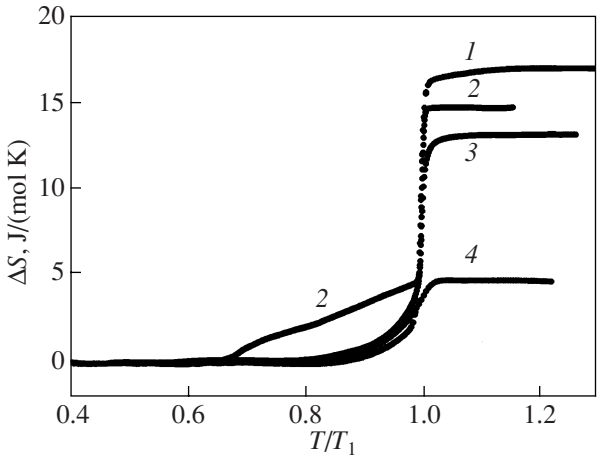

Fig. 9. Temperature dependences of the entropy of the phase transitions in the (*1*) $(NH_4)_3WO_3F_3$, (*2*) $(NH_4)_3MoO_3F_3$, (*3*) $(NH_4)_2KMoO_3F_3$, and (*4*) $(NH_4)_2KWO_3F_3$ compounds.

Recall that the results of x-ray diffraction investigations of the distorted phases of the molybdenum elpasolite and cryolite differ from each other: the structure reflections are not split in the x-ray diffraction patterns of the $(NH_4)_3MoO_3F_3$ cryolite, whereas the splitting of structure reflection is characteristic of the former compound. Moreover, these crystals differ in their sensitivity to the external pressure. Both experimentally revealed facts undeniably suggest that the specific features of the mechanism of structural distortions in these compounds differ from each other. Possibly, this is associated with different contents of tetrahedral cations in the structures. As was demonstrated above, the ammonium cations at the 4*b* positions in the cryolite structure are necessarily disordered and, in this case, the disordering of the tetrahedra at the 8*c* positions is most likely hindered. In the elpasolite structure, the ammonium cations at the 8*c* positions can also contribute to the mechanism of structural distortions. The vertices of the ammonium cation are located on the threefold axes, and, hence, the N–H…F(O) bonds can be disordered over three positions. As a result, the change in the entropy should be $2R\ln 3 = 18.3$ J/(mol K). However, this consideration holds true only for the structure of $A_2A'MX_6$ elpasolites with all *X* atoms of the same type. In this structure, each ammonium ion is surrounded by 12 crystallographically equivalent *X* atoms. All hydrogen bonds N–H…*X* are equivalent, and the probability of occupation of each of the three positions of the H atoms is identical. In the oxyfluorides under consideration, there are two variants of the arrangement of the F and O atoms. In the first case (*cis* configuration), the opposite faces of the octahedron are formed by atoms of the same type (symmetry C_{3v}). In the second case (*trans* configuration), each face of the octahedron is formed by two atoms of one type and one atom of another type (symmetry C_{2v}). Since the F (O) atoms

are statistically disordered in the structure, we can assume with a high probability that the set of 12 F (O) atoms surrounding the tetrahedron in the $(NH_4)_2KMoO_3F_3$ crystal can be random. As a consequence, the hydrogen bonds formed with the F (O) atoms belonging to one face of the octahedron appear to be nonequivalent and the change in the entropy due to their ordering can be considerably smaller than the limiting value equal to $2R\ln 3$. Certainly, this is only a hypothesis and its verification calls for neutron diffraction investigation of the initial and distorted phases.

7. CONCLUSIONS

Thus, the results of the performed investigations of the thermal properties and the structure of $(NH_4)_3MoO_3F_3$ crystals and their comparative analysis with the data previously obtained for the $(NH_4)_2KMoO_3F_3$, $(NH_4)_3WO_3F_3$, and $(NH_4)_2KWO_3F_3$ compounds allowed us to make the following inferences.

Ammonium-containing molybdenum oxyfluorides have cubic symmetry with space group $Fm\bar{3}m$.

Unlike tungsten compounds, in molybdenum compounds, the presence of tetrahedral cations in the structure does not lead to a violation of the relationship between the temperatures of transitions from the cubic phase (revealed previously in the study of oxyfluorides with atomic cations): these temperatures in cryolites are considerably higher than those in elpasolites. The $(NH_4)_2KMoO_3F_3$ and $(NH_4)_3MoO_3F_3$ compounds undergo first-order phase transitions.

The loss of stability of the cubic phases in the molybdenum elpasolite and molybdenum cryolite is accompanied by close changes in the entropy in contrast to the tungsten compounds, for which the entropies of the corresponding phase transitions differ substantially.

The thermal parameters and the electron density distribution of the F (O) atoms in the molybdenum oxyfluorides correspond to a higher occupancy of the 24*e* position as compared to the tungsten compounds. This is in reasonable agreement with the calorimetric data.

A different sensitivity of the molybdenum oxyfluorides to the hydrostatic pressure indicates that there are specific features of the mechanisms of the phase transitions in the elpasolite and cryolite structures.

It was experimentally demonstrated that reliable results can be obtained when measuring the permittivity with the use of quasi-ceramic samples prepared by pressing powders without subsequent heat treatment.

It was established that the $(NH_4)_3MoO_3F_3$ cryolite undergoes ferroelectric and ferroelastic phase transitions at temperatures T_1 and T_2, respectively.

The analysis of all experimental data for tungsten and molybdenum oxyfluorides demonstrated that tetrahedral cations and quasi-octahedral anions make different contributions to the mechanism of structural distortions.

ACKNOWLEDGMENTS

We would like to thank S.V. Meln'nikova for performing the observations of the samples with a polarizing optical microscope.

This study was supported by the Russian Foundation for Basic Research (project no. 06-02-16102), the Council on Grants from the President of the Russian Federation for the Support of Leading Scientific Schools of the Russian Federation (NSh-4137.2006.2), and the Siberian Branch of the Russian Academy of Sciences (Lavrent'ev Competition of Young Scientists Projects, grant no. 51).

REFERENCES

1. I. N. Flerov, M. V. Gorev, V. D. Fokina, A. F. Bovina, and N. M. Laptash, Fiz. Tverd. Tela (St. Petersburg) **46** (5), 888 (2004) [Phys. Solid State **46** (5), 915 (2004)].
2. I. N. Flerov, M. V. Gorev, V. D. Fokina, M. S. Molokeev, Yu. V. Boĭko, V. N. Voronov, and A. G. Kocharova, Fiz. Tverd. Tela (St. Petersburg) **48** (1), 99 (2006).
3. V. D. Fokina, I. N. Flerov, M. V. Gorev, M. S. Molokeev, A. D. Vasiliev, and N. M. Laptash, Ferroelectrics **347**, 60 (2007).
4. J. Ravez, G. Peraudeau, H. Arend, S. C. Abrahams, and P. Hagenmüller, Ferroelectrics **26**, 767 (1980).
5. I. N. Flerov, M. V. Gorev, V. D. Fokina, A. F. Bovina, M. S. Molokeev, E. I. Pogorel'tsev, and N. M. Laptash, Fiz. Tverd. Tela (St. Petersburg) **49** (1), 136 (2007) [Phys. Solid State **49** (1), 141 (2007)].
6. G. Peraudeau, J. Ravez, P. Hagenmüller, and H. Arend, Solid State Commun. **27**, 591 (1978).
7. I. N. Flerov, V. D. Fokina, M. V. Gorev, A. V. Vasiliev, A. F. Bovina, M. S. Molokeev, A. G. Kocharova, and N. M. Laptash, Fiz. Tverd. Tela (St. Petersburg) **48** (4), 711 (2006) [Phys. Solid State **48** (4), 759 (2006)].
8. S. V. Mel'nikova, V. D. Fokina, and N. M. Laptash, Fiz. Tverd. Tela (St. Petersburg) **48** (1), 110 (2006) [Phys. Solid State **48** (1), 117 (2006)].
9. B. A. Strukov and A. P. Levanyuk, *Ferroelectric Phenomena in Crystals: Physical Foundations* (Nauka, Moscow, 1983; Springer, Berlin, 1998).
10. F. Iona and G. Shirane, *Ferroelectric Crystals* (Pergamon, Oxford, 1962; Mir, Moscow, 1965).
11. A. Guyomar, G. Sebald, B. Guihard, and L. Seveyrat, J. Phys. D: Appl. Phys. **39**, 4491 (2006).
12. I. N. Flerov, M. V. Gorev, K. S. Aleksandrov, A. Tressaud, J. Grannec, and M. Couzi, Mater. Sci. Eng., B **24**, 81 (1998).
13. F. J. Brink, L. Noren, D. J. Goossens, R. L. Withers, Y. Liu, and C.-N. Xu, J. Solid State Chem. **174**, 450 (2003).

Translated by O. Borovik-Romanova